CFD MODEL BASED ANN PREDICTION OF FLAMMABLE VAPOR CLOUD FORMED BY LIQUID HYDROGEN SPILL

He, Pan.[1], Li, Xuefang.[2], Bénard, Pierre.[3], Chahine, Richard.[3]and Xiao, Jinsheng.[1, 2, 3,*]
[1] Hubei Research Center for New Energy & Intelligent Connected Vehicle and Hubei Key Laboratory of Advanced Technology for Automotive Components, School of Automotive Engineering, Wuhan University of Technology, Hubei 430070, China; panhe@whut.edu.cn (P.H.); Jinsheng.Xiao@uqtr.ca (J.X.)
[2] Institute of Thermal Science and Technology, Shandong University, Shandong 250061, China; lixf@email.sdu.edu.cn (X.L.)
[3] Hydrogen Research Institute, Université du Québec à Trois-Rivières, QC G9A 5H7, Canada; Pierre.Benard@uqtr.ca (P.B.); Richard.Chahine@uqtr.ca (R.C.)

ABSTRACT

Unintended releases can occur during the production, storage, transportation and filling of liquid hydrogen, which may cause devastating consequences. In the present work, liquid hydrogen leak is modeled in ANSYS Fluent with the numerical model validated using the liquid hydrogen spill test data. A three-layer artificial neural network (ANN) model is built, in which the wind speed, ground temperature, leakage time and leakage rate are taken as the inputs, the horizontal diffusion distance and vertical diffusion distance of combustible gas as the outputs of the ANN. The representative sample data derived from the detailed calculation results of the numerical model are selected via the orthogonal experiment method to train and verify the back propagation (BP) neural network. Comparing the calculation results of the formula fitting with the sample data, the results show that the established ANN model can quickly and accurately predict the horizontal and vertical diffusion distance of flammable vapor cloud relatively. The influences of four parameters on the horizontal hazard distance as well as vertical hazard height are predicted and analyzed in the case of continuous overflow of liquid hydrogen using the ANN model.

1.0 INTRODUCTION

Energy development is the forerunner of social development. To solve the growing serious problem of the energy crisis, greenhouse effect and environmental pollution, people are trying to find renewable and clean energy to replace fossil fuels. As a feasible technical route to promote global energy transitions, the development of hydrogen energy has gained international attention. Hydrogen energy, a dispensable part of the clean transformation of the energy industry, has been widely used in a host of fields, such as aerospace, ferrous metallurgy, chemical industry and military, etc. Indeed, it presents great application value in cold chain transportation, medical treatment, energy storage and other fields [1]. In contrast with gas hydrogen, liquid hydrogen has obvious advantages in the storage and transportation of large-scale development of the hydrogen energy industry. When the liquid hydrogen tube or storage container is ruptured due to uncontrollable factors, the leaked liquid hydrogen will quickly evaporate and mix with the ambient air to form a flammable and explosive hydrogen cloud [2], which will cause a very harmful explosion and fire if encountered with a fire source. Therefore, it's essential for the numerical simulation of the leakage and diffusion process of liquid hydrogen. And the analysis and prediction of flammable vapor cloud are of great significance to determine the risk range, guide the emergency disposal of accidents, and push forward the development of hydrogen energy applications.

There are many research institutions in the world carrying out experimental research on the leakage and evaporation of liquid hydrogen and the diffusion of hydrogen. As early as 1981, the National Aeronautics and Space Administration (NASA) [3,4] conducted seven experiments on liquid hydrogen release in the open desert space of White Sands Test Facility (WSTF). Various instruments were used to record real-time data such as turbulence level, temperature, hydrogen concentration in the air, and track the dynamic diffusion process of visible clouds. The experimental results preliminarily revealed that the main factors affecting the movement of hydrogen cloud include heat transfer and turbulence, and the removal of cofferdam can promote the diffusion and evaporation of liquid hydrogen. The other

two typical liquid hydrogen leakage experiments were carried out by Federal Institute for Materials Research and Testing (BAM) [5] and Health and Safety Laboratory (HSL) [6]. The former simulated the complex behavior of accidental liquid hydrogen leakage and spread between buildings. The latter accomplished an effective experiment on the liquid hydrogen leakage caused by the failure of the transmission joint.

In light of the huge risks and expensive costs that come with liquid hydrogen leakage experiments, more researchers dedicated to the relevant theoretical and numerical simulation research. Sklavounos and Rigas et al [7] simulated the large-scale liquid hydrogen spill test process, and found that the diffusion of liquid hydrogen leakage at low temperature was heavy gas diffusion, which aggravated the damage to the ground. Ichard et al [8] studied the effect of different mass fractions of liquid hydrogen on the experiment, and it was found that air condensation significantly affected the temperature field around the liquid hydrogen leakage. Giannissi et al [9] conducted a survey of the small-scale liquid hydrogen leakage experiment by using the CFD tool ADREA-HF, and found that the diffusion process of hydrogen can be better simulated if taking the atmospheric humidity and slip effect into consideration. Schmidt et al [10] studied the influence of different liquid hydrogen release conditions and wind speed on the hydrogen concentration near the ground. The results showed that reducing the liquid hydrogen release speed promoted the upward movement of hydrogen cloud, thus eliminating the explosion risk of the ground area. Jin et al [11,12] explored various factors that affected the concentration of hydrogen cloud. From the perspective of safety, the variation of diffusion distance of downwind combustible cloud with time in horizontal, vertical and height directions were investigated under consideration of the continuous and time-limited leakage of liquid hydrogen. Shao et al. [13,14] studied the formation and diffusion of combustible hydrogen cloud in different scenes and weather conditions, and analyzed the influence of different atmospheric pressure on the displacement of combustible hydrogen cloud.

In this paper, a three-dimensional transient simulation model for leakage and diffusion of liquid hydrogen is established and then verified by experimental data. Sample data are selected from the simulation results to train and verify the machine learning model—ANN. The calculation formula of horizontal diffusion distance of flammable vapor cloud can be obtained by fitting the sample data in the software platform of Design-Expert. Compared with the fitting results of the formula, the results of neural network prediction and numerical simulation are in better agreement. Based on the comprehensive analysis, the ANN model can be used to predict the farthest horizontal and vertical diffusion distance of flammable vapor cloud in downwind under continuous leakage. The effects of ground temperature, leakage rate and wind speed on horizontal hazard distance and vertical hazard height are studied by using the ANN model.

2.0 NUMERICAL METHOD

2.1 Basic governing equations

Mixture model, a simplified multiphase flow model, can be used to simulate multiphase flow at different velocities between phases. In the process of liquid hydrogen leakage and hydrogen cloud diffusion, the gas phase (air, hydrogen) is used as the primary phase, and the liquid phase (liquid hydrogen, water) is taken as the second phase, it is assumed that both gas and liquid phases are incompressible and in thermal equilibrium, but possess different velocities, the multiphase flow is simulated by solving the three-dimensional, transient conservation equations for mixture mass, mixture momentum, mixture enthalpy, the volume fraction equation of the liquid phase and numerical expression of relative velocity. The continuity, momentum and energy equations for the mixture are expressed as:

$$\frac{\partial \rho_m}{\partial t} + \nabla \cdot (\rho_m \boldsymbol{v}_m) = 0 \tag{1}$$

$$\frac{\partial}{\partial t}(\rho_m \boldsymbol{v}_m) + \nabla \cdot (\rho_m \boldsymbol{v}_m \boldsymbol{v}_m) = -\nabla p + \nabla \cdot [\mu_m (\nabla \boldsymbol{v}_m + \nabla \boldsymbol{v}_m^T)] + \rho_m \boldsymbol{g} + \boldsymbol{F} + \nabla \cdot \left(\sum_{k=1}^{2} \alpha_k \rho_k \boldsymbol{v}_{dr,k} \boldsymbol{v}_{dr,k}\right) \tag{2}$$

$$\frac{\partial}{\partial t}\sum_{k=1}^{2}(\alpha_k\rho_k E_k) + \nabla\cdot\sum_{k=1}^{2}[\alpha_k \boldsymbol{v}_k(\rho_k E_k + p)] = \nabla\cdot(k_{\text{eff}}\nabla T) + S_E \tag{3}$$

The volume fraction equation for the liquid phase is defined as:

$$\frac{\partial}{\partial t}(\alpha_p\rho_p) + \nabla\cdot(\alpha_p\rho_p\boldsymbol{v}_m) = -\nabla\cdot(\alpha_p\rho_p\boldsymbol{v}_{\text{dr},p}) + \sum_{q=1}^{2}(\dot{m}_{qp} - \dot{m}_{pq}) \tag{4}$$

The definition of slip speed between phases adopts the form proposed by Mikko et al. [15], and the expression is:

$$\boldsymbol{v}_{pq} = \frac{\tau_p}{f_{\text{drag}}}\frac{\rho_p - \rho_m}{\rho_p}\boldsymbol{a} \tag{5}$$

The drag function f_{drag} can be described as:

$$f_{\text{drag}} = \begin{cases} 1 + 0.15\text{Re}^{0.687} & \text{Re} \le 1000 \\ 0.0183\text{Re} & \text{Re} > 1000 \end{cases} \tag{6}$$

Lee model has been widely used to simulate the phase transition of liquid hydrogen [16]. The mass transfer rate is proportional to the product of volume fraction and density of the species, and the coeff is a coefficient that must be fine-tuned and can be interpreted as a relaxation time. The modified Lee model [17] is used to calculate the mass transfer between phases and it can be described as follows:

$$\begin{aligned} &\dot{m}_{pq} = \text{coeff}\cdot\alpha_p\rho_p(T_p - T_{\text{sat}})/T_{\text{sat}}\text{, if } T_p > T_{\text{sat}} \\ &\dot{m}_{qp} = \text{coeff}\cdot\alpha_q\rho_q(T_q - \text{T}_{\text{sat}})/T_{\text{sat}}\text{, if } T_q < T_{\text{sat}} \end{aligned} \tag{7}$$

The convection-diffusion equation used to solve the mass fraction of species *i* in the gas phase is:

$$\frac{\partial}{\partial t}(\alpha_q\rho_q Y_{q^i}) + \nabla\cdot(\alpha_q\rho_q\boldsymbol{v}_q Y_{q^i}) = -\nabla\cdot\alpha_q\left[-(\rho D_{i,m} + \frac{\mu_t}{Sc_t})\nabla Y_i\right] + (\dot{m}_{p^j q^i} - \dot{m}_{q^i p^j}) \tag{8}$$

The k and ε are calculated following the transport equations:

$$\frac{\partial}{\partial t}(\rho k) + \frac{\partial}{\partial x_{\text{j}}}(\rho k u_{\text{j}}) = \frac{\partial}{\partial x_{\text{j}}}\left[\left(\mu + \frac{\mu_{\text{i}}}{\sigma_{\text{k}}}\right)\cdot\frac{\partial k}{\partial x_{\text{j}}}\right] + G_{\text{k}} + G_{\text{b}} - \rho\varepsilon \tag{9}$$

$$\frac{\partial}{\partial t}(\rho\varepsilon) + \frac{\partial}{\partial x_{\text{j}}}(\rho\varepsilon u_{\text{j}}) = \frac{\partial}{\partial x_{\text{j}}}[(\mu + \frac{\mu_{\text{i}}}{\sigma_\varepsilon})\cdot\frac{\partial\varepsilon}{\partial x_{\text{j}}}] + \rho C_1 E\varepsilon - \rho C_2\frac{\varepsilon^2}{k+\sqrt{\nu\varepsilon}} + C_{1\varepsilon}\frac{\varepsilon}{k}C_{3\varepsilon}G_{\text{b}} \tag{10}$$

The wind field in the atmospheric boundary layer which uses the exponential wind profile recommended by Architectural Institute of Japan (AIJ) [18] is adopted:

$$u(z) = u_0(\frac{z}{z_0})^{\Phi} \tag{11}$$

The corresponding turbulent kinetic energy and turbulent diffusivity can be expressed as:

$$k(z) = \frac{3}{2}[u(z)I(z)]^2 \tag{12}$$

$$\varepsilon(z) = C_\mu^{3/4}k(z)^{1.5}/l(z) \tag{13}$$

2.2 Geometric model and simulation conditions

Based on NASA Test 6 of the liquid hydrogen spill experiments [4], the geometric model with a total spatial scale of 220 m (x) × 70 m (y) × 90 m (z) is constructed and y = 0 is used as geometric symmetry plane to improve computing efficiency. The calculation domain and boundary conditions are schematically demonstrated in Fig. 1. The ground is set as the non-slip wall, the material of the ground is selected as compacted sand and the thickness is 2 m, with the heat capacity, density and thermal conductivity of the ground are 880 $\text{J}\cdot\text{kg}^{-1}\cdot\text{K}^{-1}$, 2371 $\text{kg}\cdot\text{m}^{-3}$ and 1.13 $\text{W}\cdot\text{m}^{-1}\cdot\text{K}^{-1}$, respectively. The inner diameter, outer diameter and height of the semicircular cofferdam are 9.1 m, 9.6 m and 0.61 m, respectively. The leakage pipeline is simulated as a cube of 0.5 m (x) × 0.25 m (y) × 0.5 m (z), of which the surface beneath is set as the leakage source of liquid hydrogen, and the Center of the leakage source is located at the coordinates of (20.25, 0, 0.5). Also, the liquid hydrogen mass fraction of 98 % at the source is adopted according to the comparison between the numerical results and the experimental results. The boundary conditions on the left and right sides of the computational domain are set as velocity inlet and pressure outlet respectively. In addition, symmetrical boundary conditions

are adopted at the front, back and top, and the flux of all flow variables is zero in the plane of symmetry. The specific simulation conditions are listed in Table 1.

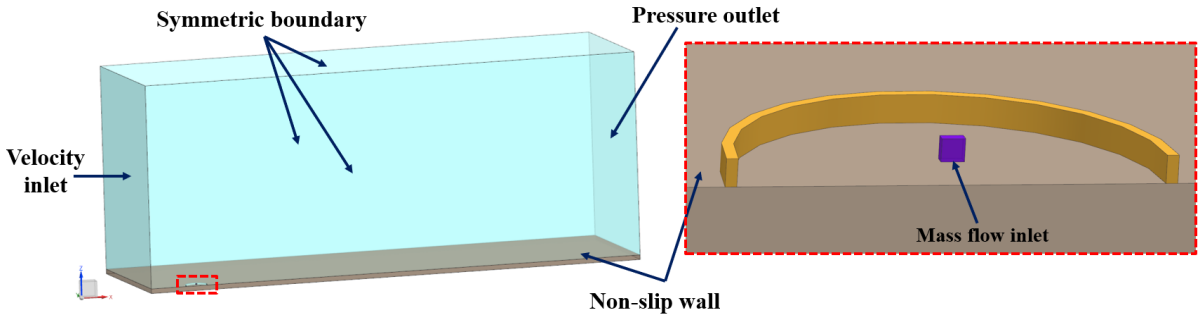

Figure 1. Schematic diagram of calculation domain and boundary conditions

Table 1. Simulation conditions of liquid hydrogen leakage

Parameter	Value
Leakage rate (kg/s)	4.76
Leakage time (s)	38
Flash mass fraction of liquid hydrogen (100%)	2
Liquid hydrogen temperature (K)	20
Liquid hydrogen saturation temperature (K)	20.35
Wind speed at 10 m in height (m/s)	2.2
Atmospheric boundary layer height (m)	250
Ground roughness coefficient	0.1
Ground temperature (K)	288
Air temperature (K)	288
Ambient relative humidity (100%)	29
Water dew point (K)	270

2.3 Meshing and independence analysis

ICEM is used to divide structured hexahedral gird on the region of calculation. As Fig. 2 displays, the grids near the leak source are refined locally by adopting an O-shaped division. The minimum and maximum grid sizes of the encrypted area are 0.1 m and 0.9 m respectively, the global maximum grid size is 1.5m, with the grid expansion rate is not greater than 1.2. ICEM mainly evaluates the quality of the grid by angle, aspect ratio, and determinant [19], the quality of the grid divided in this paper meets the basic computing requirements of Fluent software by the assessment. The variation of hydrogen concentration at the monitoring point (1 m in height, 18.3 m in downwind of leakage source) is chosen for the grid independence test. The results of the independence test are presented in Fig. 3. The relative error between the volume fraction of hydrogen based on 947,247 cells and 801,248 cells does not exceed 3%. Taking the astringency and computational efficiency of mesh into consideration, the mesh with 801,248 cells is adopted in the following simulation.

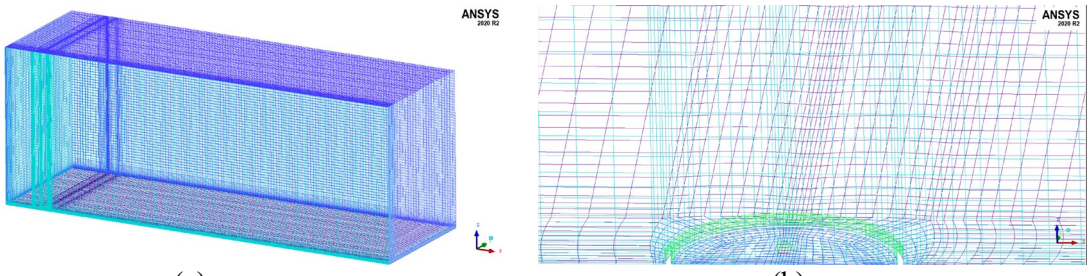

(a) (b)

Figure 2. Grid of fluid domain (a) and zoom view of liquid hydrogen jet region (b).

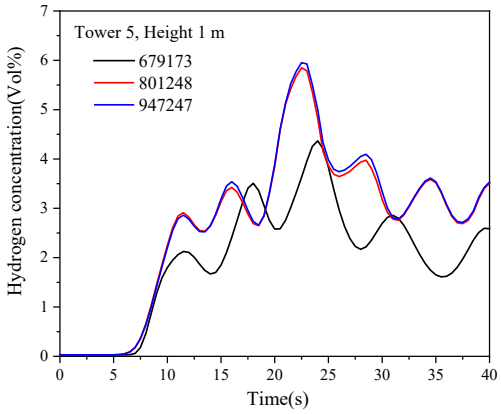

Figure 3. Grid independence assessment

3.0 MODEL CALCULATION AND VERIFICATION

The commercial Computational Fluid Dynamics (CFD) software ANSYS Fluent 2020R2 is used for simulation analysis. The User-Defined Function (UDF) of AIJ exponential wind speed, turbulent kinetic energy and turbulent diffusivity are compiled. For the simple two-phase mixing problem, the Mixture Model is better adopted to simplify the calculation in comparison with the Volume of Fluid (VOF) model and the Eulerian model. A realizable $k-\varepsilon$ turbulence model [20] with enhanced wall function is employed for modelling the turbulence. The buoyancy effect is fully considered, and the gravity option and component transportation are turned on. The values of the evaporation coefficient and condensation coefficient used in the simulation are 5 and 0.25, respectively. The process is solved with the time step of 0.01s, and the convergence criterion is 10^{-3}.

The experimental results of more comprehensive Test 6 in the seven NASA experiments of liquid hydrogen release were used to verify the simulation model. The relative deviation can be illustrated in three aspects, i.e., the distance of the hydrogen cloud front separating from the ground, the farthest distance in the downwind and in the height direction of the dilute hydrogen cloud (8% volume fraction of hydrogen). The experimental and simulated images of hydrogen concentration at 20.94s are depicted in Fig. 4.

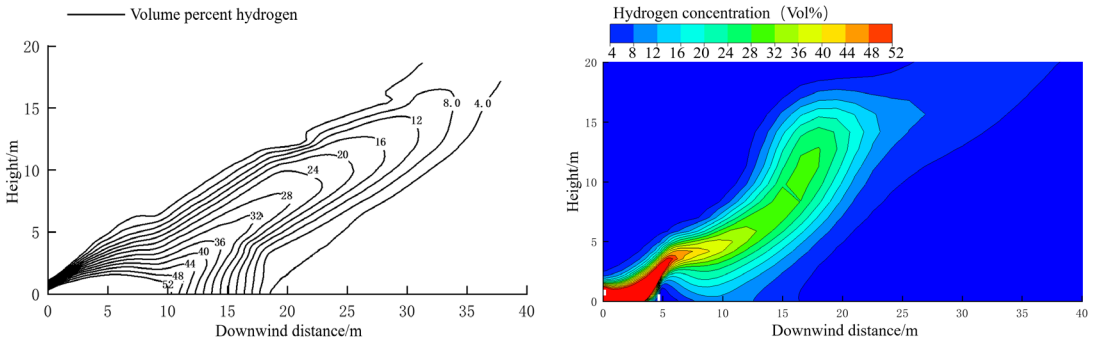

(a) (b)

Figure 4. Hydrogen concentration contour on the symmetric plane at 20.94 s. (a) Experimental result. (b) Simulation result.

In Table 2, it's obvious that the deviation of the height direction is below 6%, while the deviation of the farthest distance in the downwind of the dilute hydrogen cloud achieves 20.6%. The main reasons for the deviation are as follows: in the experiment, part of the liquid hydrogen will penetrate into the sand, which will improve the evaporation rate of liquid hydrogen; there is no specific value for the flash mass fraction of liquid hydrogen at the leakage outlet; the phase transition of oxygen and nitrogen is not studied in the model, the condensation of oxygen and nitrogen near the liquid hydrogen outlet will release heat, thus accelerating the evaporation of liquid hydrogen and diffusion of

hydrogen; the fickle wind and turbulence in the experiment cannot be accurately predicted by simulation; and besides, the influence of radiation heat transfer, uneven ground, pipeline for transporting liquid hydrogen and other obstacles is not considered in the model.

Table 2. The relative deviation of simulation and experiment

Parameter	Simulation	Experiment	Relative deviation
the distance of the hydrogen cloud front separating from the ground (m)	16.46	18.40	10.5%
the farthest distance of the dilute hydrogen cloud in the downwind direction (m)	26.89	33.87	20.6%
the farthest distance of the dilute hydrogen cloud in the height direction (m)	17.62	16.68	5.6%

The concentration variation of the monitoring point A (29.35, 0, 1) near the leakage source and the monitoring point B (38.55, 0, 1) away from the source of leakage are collected, and the experiment data originate from the sample bottle and the predicted values obtained by Venetsanos et al. [21] through ADREA-HF are compared. The variety law of hydrogen concentration at the monitoring point is represented in Fig. 5, the hydrogen concentration of simulation and experiment qualitatively have similar trends but there is a consistent difference in the maximum values. In the simulation, the wind speed and direction at the entrance of the calculation domain do not change and as a consequence of a more stable concentration variation in time compared to experiments. Furthermore, the predicted high concentration gas cloud (volume fraction of hydrogen is not less than 36%) is located in the area of 15 m downwind and 5 m high near the leakage source, which is consistent with the experimental results. In conclusion, the numerical model established in this paper can be used to analyze the atmospheric diffusion behavior of liquid hydrogen leakage.

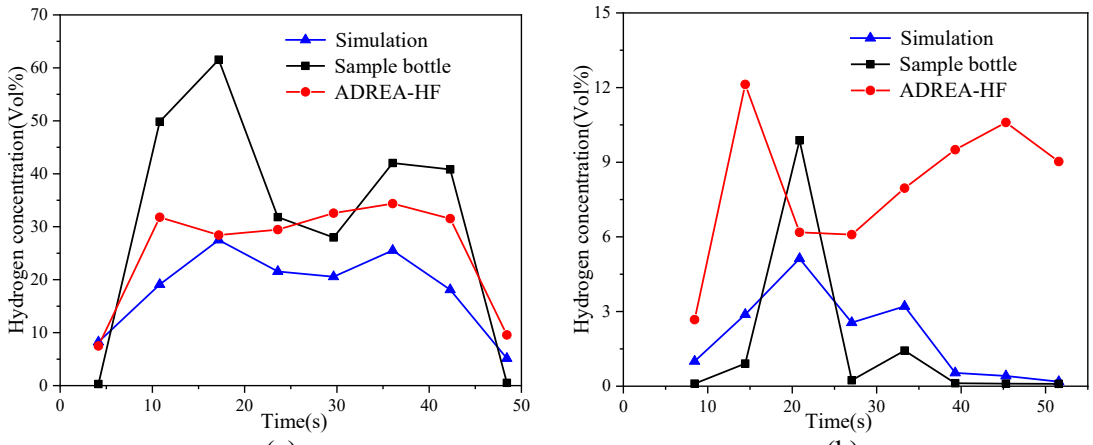

Figure 5. Hydrogen concentration variation of monitoring points. (a) Point A. (b) Point B.

4.0 ARTIFICIAL NEURAL NETWORK

Artificial neural network (ANN), a kind of machine learning algorithms, constructs a mathematical model to estimate the function by imitating biological neural network, it has the characteristics of excellent adaptive learning and non-linear fitting, and can be applied to sensitivity analysis and optimization of parameter, analysis and prediction of data [22]. Back propagation (BP) neural network is a feed forward neural network based on error back Propagation algorithm, in the feedback process, the error will be back propagated to all neurons in each layer, and the connection weight and the threshold of neurons will be adjusted according to the error for optimizing the network.

4.1 Training and validation of BP neural network

It can be seen from Fig. 6 that the three layers BP neural network is built. Four factors having a powerful influence on the leakage and diffusion of liquid hydrogen, including wind speed, ground temperature, leakage time and leakage rate, are selected as the inputs of the neural network, and the horizontal and vertical diffusion distance of flammable vapor cloud are adopted as the outputs. The training and test data originate from calculative results of the Fluent simulation model established in this paper section 3 with different initial parameters. The designed level values are presented in Table 3. For the sake of great efficiency, the orthogonal experiment is used to choose the 44 sets of representative data from all permutations and combinations, 44 sets of data were randomly allocated into the training set and test set in the ratio of 3:1 for the training and validation of neural network.

Table 3. Parametric level values used in ANN.

Parameter	Level value
Wind speed (m/s)	1.8, 2.0, 2.2, 2.4, 2.6, 2.8
Leakage rate (kg/s)	2, 3, 4, 5, 6
Leakage time (s)	10, 15, 20, 25, 30, 35, 40
Ground temperature (K)	286, 288, 290, 292

Selecting the appropriate number of layers and nodes in the hidden layer will greatly affect the fitting effect of the neural network. Table 4 lists the parameter setting of the ANN. The single hidden layer is used because of the relatively simple dataset. Generally, the number of nodes in the hidden layer should be less than twice the number of input parameters, and when it is 4, the mean square error (MSE) reaches the minimum with value is 8.77×10^{-3} . The learning rate of neural network model picked according to experience is 1×10^{-4}. Activation function refers to the law that neurons generate output signals under the action of input signals, its function is mainly to increase the nonlinear fitting characteristics of neurons [23]. The hidden layer is expressed by hyperbolic tangent S-type Tansig function, and the output layer adopts the default Purelin transfer function of MATLAB software.

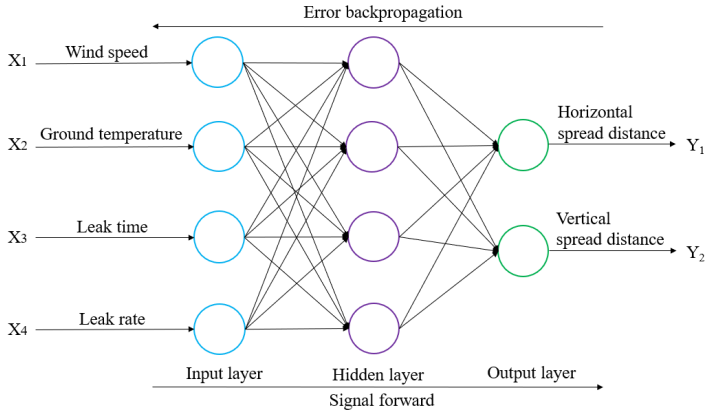

Figure 6. Structure diagram of three-layer neural network model

Table 4. Parameters setting of ANN

Parameter	ANN
Number of nodes in the input layer	4
Number of hidden layers	1
Number of nodes in the hidden layer	4
Number of nodes in the output layer	2
The activation functions of the hidden layer	Tansig
The activation functions of the output layer	Purelin
Learning rate of neural network	1×10^{-4}

The regression correlation coefficient between the Fluent simulation results and the ANN prediction output is illustrated in Fig. 7. It could be found that the correlation coefficients of the training set, the test set and the validation set are more than 0.9, and the overall correlation coefficient of the neural network reaches 0.98958. Fig. 8 shows the comparison between ANN prediction and test data. The percentage errors of vertical diffusion distance between predicted values and test data are within 10%. Among the 11 test points of horizontal diffusion distance, the prediction error of 2 test points is more than 7 m. It can be concluded that the ANN has a good fitting and prediction for horizontal and vertical diffusion distance of combustible gas.

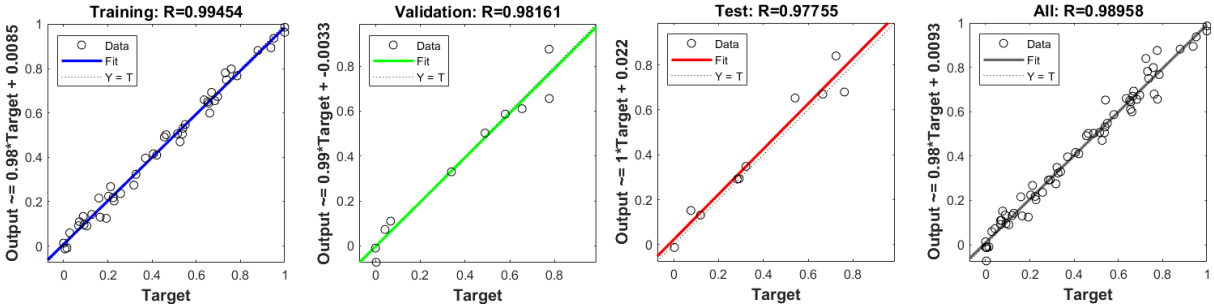

Figure 7. Regression correlation coefficient between predicted output and simulation results

The calculation formula of horizontal and vertical diffusion distance of flammable vapor cloud can be obtained by fitting the sample data in the software platform of Design-Expert. The comparison of the mathematical models employed for the fitting equation is shown in Table 5. P-value is used to detect the significance of the model, and the closer its value is to zero, the higher the correctness of the model. The linear equation is adopted to fit the horizontal diffusion distance, while quadratic equation is more suitable for fitting the vertical diffusion distance. Analysis of variance is used to remove the non-significant factor in the fitting equation, and the R-squared of the fitting formula for the horizontal and vertical diffusion distance is 0.9545 and 0.9945, respectively. The regression equations obtained are as follows.

$$\text{Horizontal diffusion distance} = -600.29 + 12.18u_0 + 2.27\dot{m}_{pq} + 2.25t + 2.02T \quad (14)$$

$$\text{Vertical diffusion distance} = -33.2 + 2.77u_0 + 5.6\dot{m}_{pq} + 4.68t - 0.69u_0t + 0.25\dot{m}_{pq}t - 0.00197tT - 0.88\dot{m}_{pq}^2 - 0.05t^2 \quad (15)$$

Table 5. The comparison of the mathematical models

Source of p-value	Horizontal diffusion distance	Vertical diffusion distance
Linear	<0.0001	0.0231
Dual Factor	0.0255	0.1815
Quadratic	0.4417	<0.0001

The test set data are also used to verify the fitting formula. Compared with the simulation data, the evaluation results of ANN prediction and formula prediction are demonstrated in detail as Table 6. The root mean square error (RMSE) and the maximum relative error (MRE) of the ANN prediction results are smaller than the formula calculation results, whether the horizontal or vertical diffusion distance of flammable vapor cloud. Moreover, the speed of ANN prediction is superior in comparison with the speed of numerical simulation. We can conclude that the established ANN model can quickly and relatively accurately predict the horizontal and vertical diffusion distance of flammable vapor cloud.

Table 6. Evaluation of ANN prediction and formula prediction

Prediction methods	RMSE	MRE
ANN (the horizontal diffusion distance of flammable vapor cloud)	5.18	13.8%
Fitting formula (the horizontal diffusion distance of flammable vapor cloud)	5.28	15.4%
ANN (the vertical diffusion distance of flammable vapor cloud)	2.21	9.0%
Fitting formula (the vertical diffusion distance of flammable vapor cloud)	2.30	12.9%

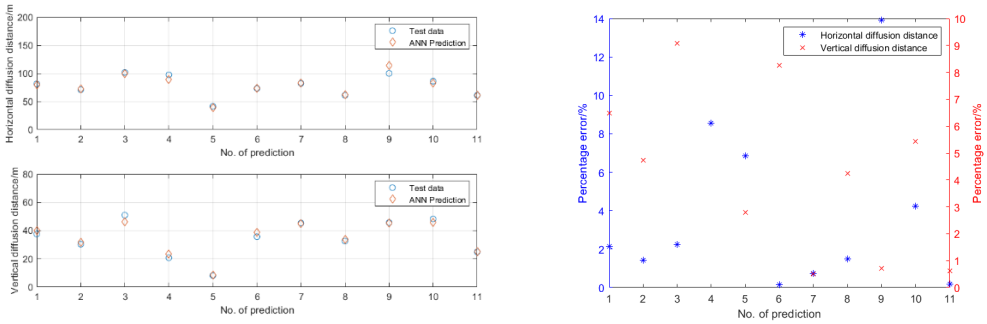

(a) (b)

Figure 8. Comparison between predicted and simulated values. (a) The result of ANN prediction. (b) The percentage errors of horizontal and vertical diffusion distance.

4.2 Prediction of hazard distance using ANN

The leaked liquid hydrogen will quickly mix with the surrounding air to form flammable and explosive hydrogen clouds, which will pose a serious security threat to the surrounding personnel and equipment, it is important to limit the dangerous range of hydrogen cloud with the standard of 4% volume fraction of hydrogen. The atmospheric diffusion behavior of hydrogen cloud is affected by many factors, such as atmospheric boundary layer wind field, atmospheric humidity and temperature, ground heat transfer condition, leakage source condition and so on. It is very complex to deduce the expansion distance of combustible vapor cloud theoretically, and the accuracy of empirical formula fitting is limited. In this case, utilizing the ANN model to make predictions is a better method, and the horizontal and vertical farthest expansion distances in the downwind of flammable vapor cloud (4%-75% volume fraction of hydrogen) are taken as horizontal hazard distance and vertical hazard height.

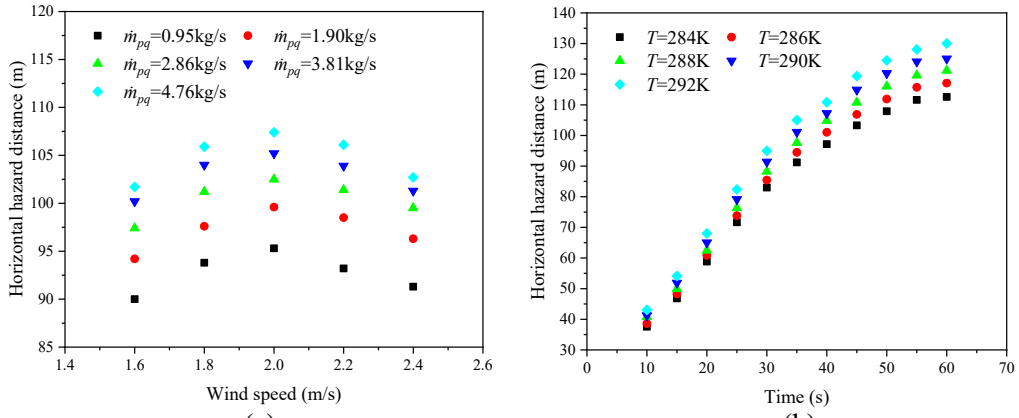

(a) (b)

Figure 9. Variations of horizontal hazard distance. (a) Different wind speeds and leakage rates(t=40s, T=288K). (b) Different leakage time and ground temperature($\dot{m}_{pq}$=4.76kg/s, u_0=2.2m/s).

The variations of horizontal hazard distance under different conditions can be seen in Fig. 9. The prediction results of the ANN model indicate that the horizontal hazard distance first increases and then decreases with the augment of wind speed. If the liquid hydrogen leaks at a higher rate, the horizontal hazard distance will ascend but at a slower rate. In addition, the horizontal hazard distance is positively correlated with the leakage time of liquid hydrogen and the ground temperature.

As shown in Fig. 10, the vertical hazard height decreases rapidly with the increasing wind speed, and increases with the increased buoyancy of hydrogen cloud brought by the rising ground temperature. However, the ground temperature has a weaker influence on the vertical hazard height when at a wind speed higher than 2.4m/s, which is because the larger wind speed mainly promotes the downward movement of the hydrogen cloud. The speed of the vertical hazard height increases getting slower with the increase of the liquid hydrogen leakage time.

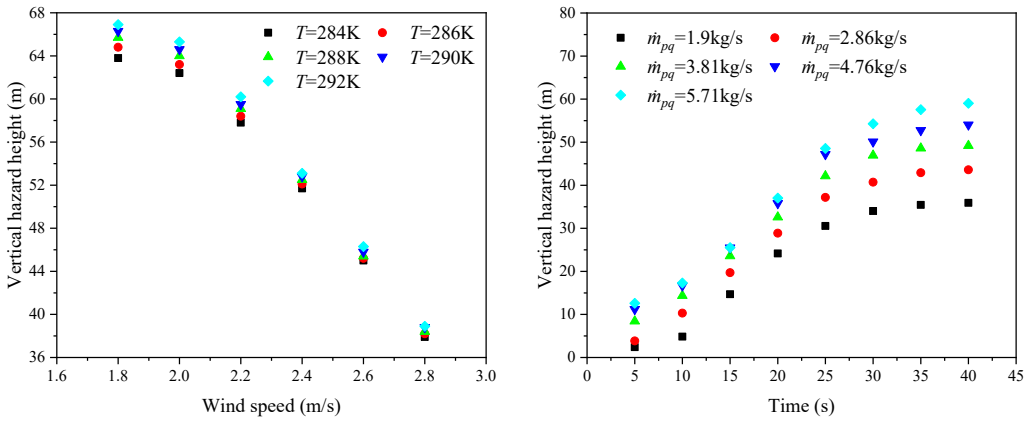

(a) (b)

Figure 10. Variations of vertical hazard height. (a) Different wind speeds and temperature (t=40s, $\dot{m}_{pq}$=4.76kg/s). (b) Different leakage time and leakage rates (T=288K, u_0=2.2m/s).

5.0 CONCLUSIONS

This work aims to study and predict the diffusion distance of flammable hydrogen cloud by using the ANN model and provide timely guidance and suggestions for risk assessment and disaster prevention. The established three-layer ANN model is trained and tested by using the detailed sample data from the numerical simulation model, and the prediction results of the fitting formula are also compared to illustrate the prediction ability of ANN. The influence of wind speed, ground temperature, leakage time and leakage rate on the horizontal hazard distance and vertical hazard height are studied adopting the ANN model. The main conclusions are drawn as:

(1) Compared with the prediction results of the fitting formula, the ANN model has a better prediction in the horizontal hazard distance and vertical hazard height of liquid hydrogen leakage, and the prediction speed is improved dozens of times in comparison with the speed of numerical simulation. The application of the ANN model will contribute to the rapid determination of dangerous regions and the guidance of emergencies in the case of liquid hydrogen leakage.

(2) The wind speed has a great influence on the diffusion distance of the flammable vapor cloud. The horizontal hazard distance begins to decrease when the reference wind speed more than 2.0m/s while the vertical hazard height decreased continuously with the increasing wind speed. It is an effective measure to increase the ambient wind speed to promote the movement of hydrogen cloud and narrow the hazard scope.

(3) Both horizontal hazard distance and vertical hazard height increase and then go to be flat with the increase of leakage time, and they are positively correlated with the leakage rate and the ground temperature. However, the variations in ground temperature obtain a limited impact on the

diffusion distance of combustible vapor cloud because of the extreme difference in temperature between liquid hydrogen and the ground.

There is still room for improvement in future studies. In the process of establishing the numerical simulation model, the phase transition of oxygen and nitrogen in the air and the accurate mass fraction of liquid hydrogen flash can be considered to optimize the model. Besides, opting for more input parameters affecting diffusion of hydrogen and sample data originating from the CFD model can effectively improve the forecast precision of the neural network model. Similarly, the ANN model can also be adopted to analyze and predict other factors in the process of liquid hydrogen leakage.

ACKNOWLEDGEMENTS

This work was supported by the financial supports from the National Natural Science Foundation of China (Project No. 51476120).

NOMENCLATURES

$\boldsymbol{a}$	particle acceleration vector of P phase, m/s^2	T_p	the temperature of P phase
coeff	relaxation time coefficient, 1/s	T_q	the temperature of Q phase
D_t	turbulent diffusivity, m^2/s	T_{sat}	saturation temperature, K
$D_{i,m}$	molecular diffusivity of species *i* in the mixture, m^2/s	u_0	wind speed at reference altitude, m/s
D_{eff}	effective diffusivity, m^2/s	$\boldsymbol{V}_{pq}$	slip velocity vector of P phase, m/s
d_p	particle diameter of P phase, m	$\boldsymbol{V}_{dr,p}$	drift velocity vector of P phase, m/s
E_k	enthalpy of phase K, J	$\boldsymbol{V}_{dr,k}$	drift velocity vector of K phase, m/s
$\mathbf{F}$	body force vector, N	$\boldsymbol{V}_m$	mixture velocity vector, m/s
f_{drag}	drag function, dimensionless	Y_k	mass fraction of K phase, dimensionless
G_k	turbulent kinetic energy due to average velocity gradient, J	Z_0	standard reference height, m
$\mathbf{g}$	gravitational acceleration, m/s^2	Z_G	atmospheric boundary layer height, m
k_{eff}	effective thermal conductivity, W/ (m • K)	Greek symbols	
k_k	thermal conductivity of K phase, W/ (m • K)	α_k	volume fraction of K phase, dimensionless
k_t	turbulent thermal conductivity, W/ (m • K)	α_p	volume fraction of liquid, dimensionless
$\dot{m}_{pq}$	mass flow rate from vapor phase (Q phase) to liquid phase (P phase), kg/ (m^3 • s)	α_q	volume fraction of gas, dimensionless
$\dot{m}_{qp}$	mass flow rate from liquid phase (P phase) to vapor phase (Q phase), kg/ (m^3 • s)	ρ_m	average density of mixture, kg/m^3
$\dot{m}_{p^j q^i}$	mass flow rate from species J in phase P to species i in phase Q, kg/ (m^3 • s)	ρ_k	density of K phase, kg/m^3
Re	Reynolds number, dimensionless	ρ_p	density of P phase, kg/m^3
S_E	other volume heat source items, J	μ_m	average viscosity of mixture, kg/(m • s)
Sc_t	turbulence Schmidt number, dimensionless	τ_p	relaxation time of P phase particles, s
t	leakage time of liquid hydrogen, s	μ_q	viscosity of P phase, kg/(m • s)
T	ground temperature, K	$\emptyset$	roughness index

REFERENCES

1. Sharma, S. and Ghoshal, S.K., Hydrogen the future transportation fuel: from production to applications, *International Journal of Hydrogen Energy*, **41**, No. 21, 2016, pp. 8992-9003.
2. Utgikar, V.P. and Thiesen, T., Safety of compressed hydrogen fuel tanks: leakage from stationary vehicles, *Technology in Society*, **27**, No. 3, 2005, pp. 315-320.
3. Chirivella, J.E. and Witkofski, R.D., Experimental results from fast 1500 gallon LH2 spills, *American Institute of Chemical Engineering*, **251**, No. 82, 1986, pp. 120-140.
4. Witcofski, R.D. and Chirivella, J.E., Experimental and analytical analyses of the mechanisms governing the dispersion of flammable clouds formed by liquid hydrogen spills, *International Journal of Hydrogen Energy*, **9**, No. 5, 1984, pp. 425-435.
5. Schmidtchen, U., Marinescu-Pasoi, L. and Verfondern, K. et al, Simulation of accidental spills of cryogenic hydrogen in a residential area, *Cryogenics*, **34**, No. S1, 1994, pp. 401-404.

6. Hall, J.E., Hooker, P. and Willoughby, D., Ignited releases of liquid hydrogen: Safety considerations of thermal and overpressure effects, *International Journal of Hydrogen Energy*, **39**, No. 35, 2014, pp. 20547-20553.
7. Sklavounos, S. and Rigas, F., Fuel gas dispersion under cryogenic release conditions, *Energy and Fuels*, **19**, No. 6, 2005, pp. 2535-2544.
8. Ichard, M., Hansen, O.R., Middha, P. et al, CFD computations of liquid hydrogen releases, *International Journal of Hydrogen Energy*, **37**, No. 22, 2012, pp. 17380-17389.
9. Giannissi, S.G., Venetsanos, A.G., Markatos, N. et al, CFD modeling of hydrogen dispersion under cryogenic release conditions, *International Journal of Hydrogen Energy*, **39**, No. 28, 2014, pp. 15851-15863.
10. Schmidt, D., Krause, U. and Schmidtchen, U., Numerical simulation of hydrogen gas releases between buildings, *International Journal of Hydrogen Energy*, **24**, No. 5, 1999, pp. 479-488.
11. Liu, Y., Wei, J., Lei, G., Wang, T., Lan, Y., Chen, H. and Jin, T., Modeling the development of hydrogen vapor cloud considering the presence of air humidity, *International Journal of Hydrogen Energy*, **44**, No. 3, 2019, pp. 2059-2068.
12. Jin, T., Liu, Y., Wei, J., Zhang, D., Wang, X., Lei, G., Wang, T., Lan, Y. and Chen, H., Numerical investigation on the dispersion of hydrogen vapor cloud with atmospheric inversion layer, *International Journal of Hydrogen Energy*, **44**, No. 41, 2019, pp. 23513-23521.
13. Tang X., Pu L., Shao X., Lei G., Li Y., Wang X. Dispersion behavior and safety study of liquid hydrogen leakage under different application situations[J]. *International Journal of Hydrogen Energy*,**45**, No. 55, 2020, pp. 31278-31288.
14. Shao X., Pu L., Li Q., Li Y. Numerical investigation of flammable cloud on liquid hydrogen spill under various weather conditions[J]. *International Journal of Hydrogen Energy*, **43**, No. 10, 2018, pp. 5249-5260.
15. Manninen, M., Taivassalo, V. and Kallio, S., On the mixture model for multiphase flow, VTT Publications 288, Technical Research Center of Finland, 1996.
16. Liu Z, Li Y, Zhou G. Study on thermal stratification in liquid hydrogen tank under different gravity levels [J]. *International Journal of Hydrogen Energy*, 43，No. 19，2018, pp. 9369-9378.
17. Lee. W.H., A pressure iteration scheme for two-phase flow modeling, Los Alamos National Laboratory: LA-UR-79-975, 1979.
18. Tominaga, Y., Mochida, A., Yoshie, R. et al, AIJ guidelines for practical applications of CFD to pedestrian wind environment around buildings, *Journal of wind engineering and industrial Aerodynamics*, **96**, No. 10, 2008, pp. 1749-1761.
19. Hu K., Li Z., Detailed explanation of ANSYS ICEM CFD engineering example, 2014, People's Posts and Telecommunications Press, Beijing.
20. Shih, T., Liou, W., Shabbir, A. et al, A new k-eddy viscosity model for high Reynolds number flows, *Computers Fluids*, **24**, No. 3, 1995, pp. 227-238.
21. Venetsanos, A.G. and Bartzis, J.G., CFD modeling of large-scale LH2 spills in open environment, *International Journal of Hydrogen Energy*, **32**, No. 13, 2007, pp. 2171-2177.
22. Aida, F., Ibrahim, D. and Greg, F.N., Multi-objective optimization of an experimental integrated thermochemical cycle of hydrogen production with an artificial neural network, *International Journal of Hydrogen Energy*, **45**, No. 46, 2020, pp. 24355-24369.
23. Zhang Z., Neural network control and MATLAB simulation, 2011, Harbin Institute of Technology Press, Harbin.